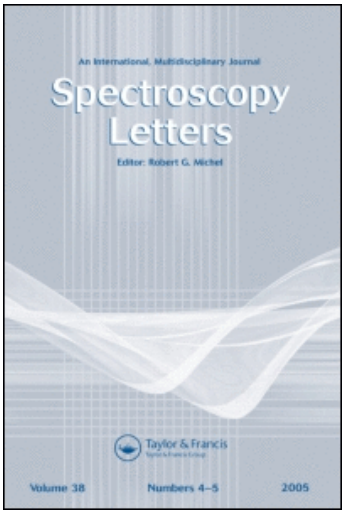

Spectroscopy Letters
Publication details, including instructions for authors and subscription information:
http://www.informaworld.com/smpp/title~content=t713597299

Prediction of Cassava Starch Edible Film Properties by Chemometric Analysis of Infrared Spectra

N. M. Vicentini[a]; N. Dupuy[b]; M. Leitzelman[b]; M. P. Cereda[c]; P. J. A. Sobral[d]
[a] Centro de Raízes e Amidos Tropicais (CERAT), Universidade Estadual Paulista, Botucatu (SP), Brazil [b] Laboratoire GOAE, UMR 6171, case 561, Université d'Aix-Marseille III, Marseille, France [c] Programa de Pós-Graduação em Desenvolvimento Local, Universidade Católica Dom Bosco, Mato Grosso do Sul, Brazil [d] ZAZ-FZEA-USP, Pirassununga (SP), Brazil

To cite this Article Vicentini, N. M. , Dupuy, N. , Leitzelman, M. , Cereda, M. P. and Sobral, P. J. A.(2005) 'Prediction of Cassava Starch Edible Film Properties by Chemometric Analysis of Infrared Spectra', Spectroscopy Letters, 38: 6, 749 — 767
To link to this Article: DOI: 10.1080/00387010500316080
URL: http://dx.doi.org/10.1080/00387010500316080

Spectroscopy Letters, 38: 749–767, 2005

ISSN 0038-7010 print/1532-2289 online
DOI: 10.1080/00387010500316080

Taylor & Francis
Taylor & Francis Group

Prediction of Cassava Starch Edible Film Properties by Chemometric Analysis of Infrared Spectra

N. M. Vicentini
Centro de Raízes e Amidos Tropicais (CERAT), Universidade Estadual Paulista, Botucatu (SP), Brazil

N. Dupuy and M. Leitzelman
Laboratoire GOAE, UMR 6171, Université d'Aix-Marseille III, Marseille, France

M. P. Cereda
Programa de Pós-Graduação em Desenvolvimento Local, Universidade Católica Dom Bosco, Mato Grosso do Sul, Brazil

P. J. A. Sobral
ZAZ-FZEA-USP, Pirassununga (SP), Brazil

Abstract: Cassava starch has been shown to make transparent and colorless flexible films without any previous chemical treatment. The functional properties of edible films are influenced by starch properties, including chain conformation, molecular bonding, crystallinity, and water content. Fourier-transform infrared (FTIR) spectroscopy in combination with attenuated total reflectance (ATR) has been applied for the elucidation of the structure and conformation of carbohydrates. This technique associated with chemometric data processing could indicate the relationship between the structural parameters and the functional properties of cassava starch–based

Received 8 May 2004, Accepted 18 March 2005
This paper was by special invitation as a contribution to a special issue of the journal entitled "Quantitative Vibrational Spectrometry in the 21st Century." This special issue was organized by Professor Miguel de la Guardia, Professor of Analytical Chemistry at Valencia University, Spain.

Address correspondence to N. Dupuy, Laboratoire GOAE, UMR 6171, case 561, Université d'Aix-Marseille III, 13397, Marseille cedex 20, France. E-mail: nathalie.dupuy@univ.u-3mrs.fr

edible films. Successful prediction of the functional properties values of the starch–based films was achieved by partial least squares regression data. The results showed that presence of the hydroxyl group on carbon 6 of the cyclic part of glucose is directly correlated with the functional properties of cassava starch films.

Keywords: Cassava, chemometric analysis, edible film, Fourier-transform infrared spectroscopy, starch

INTRODUCTION

Starch is a complex homopolymer of α-D-glucose units constituted by amylose and amylopectin. Starches from different botanic origins, such as potato, corn, wheat, and rice, natural and modified, have been used mainly in the manufacture of edible coatings[1,2] and films.[3–11]

Another starch source not yet well explored for edible film technology is the cassava (*Manihot esculenta* C.). Cassava is a tropical root, produced in various countries (e.g., Brazil, Thailand, etc.); normally, cassava roots contain 50–70% water, 20–32% starch, and trace quantities ($<2\%$) of protein and lipids.[12] Cassava starch is able to form transparent coatings[13–16] and flexible films[17,18] without previous chemical treatment nor plasticizer.

The main step in film production is thermal treatment of the starch suspension (i.e., gelatinization). During the gelatinization, the starch granules tend to rupture, and the amylose tends to leach out. After the gelatinization, during the film drying, amylose chains have a tendency to orient themselves in a parallel fashion and approach each other closely enough to permit hydrogen bonding between hydroxyl groups.[19]

The functional properties of the edible films are influenced by several factors, including extrinsic factors such as relative humidity (RH) and temperature, and intrinsic ones such as composition, mainly plasticizers (contents and characteristics) and biopolymers.[7] Some characteristics of biopolymers that influence the properties of films are molecular weight, chain conformation, molecular bonding, and crystallinity.[20–25]

The technique of Fourier-transform infrared (FTIR) spectroscopy in combination with attenuated total reflectance (ATR) has been applied for the elucidation of the structure and conformation of carbohydrates.[26,27] The infrared (IR) spectrum of starch has been shown to be sensitive to changes in structure on a molecular level (short-range order).[28,29]

Recently, FTIR spectroscopy associated with chemometric analysis was successfully employed for corn starch classification according to different chemical modifications[30] for the determination of unsaturation grade of edible oils and fats[31,32] and for expanding properties of cassava starch on the basis of the carboxyl content.[33]

Thus, the aim of this work was to study the relationship between some functional properties and the structural parameters of cassava starch–based

edible films by using Fourier-transform infrared spectroscopy associated with chemometric data processing.

EXPERIMENTAL

Cassava Starch

Commercial cassava starch supplied by an industry (Flor de Lotus Co., Brazil) was used in this study. Its characteristics were determined, in duplicate:[34] density 1.47 g/cm^3, 14.86% humidity, and 87.6% starch, of which 16.02% was amylose and 0.21% of soluble total sugars. Starch contaminants were 0.23% ash; 0.39% fiber; 0.24% total nitrogen; 0.15% lipids. The starch was used without prior preparation.

Edible Film Preparation

The films were prepared by casting technique. The filmogenic solutions (FS) were prepared with 10 (1%), 20 (2%), 30 (3%), or 40 (4%) g of starch in 1 L of distilled water heated to 70°C, in a water bath with digital control (±0.5°C) of temperature (Tecnal, TE184, USA) under constant stirring for 1 min. According to Schoch and Maywald,[35] the temperature range in that the gelatinization of the cassava starch granules occurs is 58.5°C (beginning) to 70.0°C (end). The boil of the starch/water suspension for 1 min was enough for gelatinization of all the cassava starch granules in the suspension.

The FS (20 to 70 g) were applied on Plexiglas plates (139.2 cm^2) to obtain films of different thickness. The weights were controlled (±0.01 g) with a semi-analytical balance (Marte, AS2000). The FS were dehydrated in an oven with air circulation and renewal (Marconi, MA037, USA), with proportional and integral (PI) control (±0.5°C) of temperature, at 30°C, and room relative humidity (55–65%) for 12–24 hr.

The films obtained were conditioned at 22°C and 75% of relative humidity, in desiccators containing a saturated solution of NaCl, for 6 days prior to testing. All the characterizations were carried out in a controlled environment (T = 22°C and RH = 55–65%). Before testing, the thickness of the films was measured by a digital micrometer (±0.001 mm) with a 6.4 mm-diameter probe, as the average of nine different points on each sample.

Functional Properties Determination

The functional properties studied were the mechanical properties, determined by puncture tests with a texture analyzer TA.XT2*i* (SMS, Surrey, UK),[36] the water vapor permeability (WVP), determined gravimetrically, according to a

method proposed by Gontard[37] based on the ASTM E96-80 test,[38] and color and opacity, determined using a Miniscan XE colorimeter, operated according a Hunterlab method.[39–41] All these characterizations were accomplished in a climatized room (T = 22°C and RH = 55–65%), in triplicate.

FTIR Analyses

FTIR spectra were recorded with a Perkin Elmer spectrometer (Spectrum One, USA) supplied with an attenuated total reflectance (ATR) accessory with a press in order to get a very good optical contact between the crystal and the film. The samples were analyzed by means of a diamond crystal prism manufactured by one bounce on the upper surface. The crystal geometry was a 45° triangle with mirrored angle faces. ATR spectra are shown with an absorbance scale corresponding to $\log(R_{\text{reference}}/R_{\text{sample}})$, where R is the internal reflectance of the device. The spectra were recorded between 4000 and 650 cm^{-1} with a 4 cm^{-1} spectral resolution. For each spectrum, 20 scans were co-added. The mean of three spectra of the same sample from two films was then calculated. As a reference, air was simply taken.

In the ATR experiment, the penetration depht was

$$D\text{p} = \frac{\lambda}{2\pi n_1 \left[\sin^2 \phi - \left(\frac{n_1}{n_2} \right)^2 \right]^{1/2}} \tag{1}$$

where n_1 is the refraction index of the crystal, n_2 is the refraction index of the sample, ϕ is the angle of incidence. In our case, $n_1 = 2.5$ and $\phi = 45°$. So we found approximately $D\text{p} = 0.20\lambda$.

Chemometric Method

Principal Component Analysis

Principal component analysis (PCA) is a method for extraction of the systematic variations in one data set.[42] This method can be used for classification as well as for description and interpretation.[43] PCA is oriented toward modeling the variance/covariance structure of the data matrix into a model that represents the significant variations and considers the noise as an error. The components are found during the calibration, one by one. Each principal component, called loading, represents the main systematic variation in the data set, which can be modeled after the extraction of the previous ones. Common characteristics of all the spectra are modeled in one or several principal components for which the scores are not significantly different according to the species. On the contrary, the information that differentiate the species contributes to

principal component whose scores are significant.[44] The classification may be done on the basis of the scores, and the characteristics of each species are established by the interpretation of these specific loadings. PCA is a tool for unsupervised learning (e.g., extracting regularities directly from the input data without referring to classes known in advance).

Partial Least Squares Regression

In contrast, the supervised analysis was based on the relation between the signal intensity and the modification of the sample.[45] Interference and overlapping of the absorption bands may be overcome by using powerful multicomponent analysis such as partial least squares (PLS) regression.[46,47] That allows a sophisticated statistical approach using the full spectral region rather than unique and isolated analytical bands. The algorithm is based on the ability to correlate mathematically the spectral data to a matrix property of interest while simultaneously accounting for all other significant spectral factors that perturb the spectrum.[48] It is thus a multivariate regression method that uses the full spectral region selected and is based on the use of latent variables. In the PLS procedure there are two steps: the first one is the calibration, and the second one is the prediction that tests the calibration validity. Samples of known modifications are used as calibration samples and then the modifications of an unknown sample are directly calculated using the resulting equation under the same conditions. In the current case, the PLS1 algorithm with mean centered variables was used.

The evaluation of the calibration performance is estimated by computing the standard error of calibration (SEC) after comparing the real modification with the computed one for each component. The equation for the standard error of calibration is

$$\mathrm{SEC} = \sqrt{\left(\frac{\sum_{i=1}^{N}(C_i - C_i')^2}{N - 1 - P}\right)} \tag{2}$$

where C_i is the known value, C_i' is the calculated value, N is the number of samples, and P is the number of independent variables in the regression.

On the other hand, the standard error of prediction (SEP) gives an estimation of the prediction performance during the step of validation of the calibration equation.

$$\mathrm{SEP} = \sqrt{\left(\frac{\sum_{i=1}^{M}(C_i - C_i')^2}{M - 1}\right)} \tag{3}$$

where C_i' is the calculated value by the calibration equation, and M is the number of samples in the prediction set.

The reproducibility of the signal at each wavelength is defined by the relative standard deviation (RSD) according to eq. (4):

$$\mathrm{RSD} = \left(\frac{\sigma}{x_m}\right) \times 100 \tag{4}$$

where

$$\sigma = \sqrt{\frac{\left(\sum_i^N x_i - x_m\right)^2}{N-1}} \tag{5}$$

and x_i represents the intensity of one spectrum, x_m is the average intensity of all spectra of the same sample, and N is the number of spectra.

For some chemometric applications, the spectral data were first-derived with the algorithm developed by Savitzky and Golay[49] to remove the unwanted spectral variations as offsets, and a smoothing with five points was performed. The nonderivatized spectra were not smoothed. In all cases, the spectra were maximum normalized.

The chemometric applications are performed by the UNSCRAMBLER software version 7.5 from CAMO (Computer Aided Modelling A/S, Trondheim, Norway).

Optimization of a Model

As the SEP is a standard deviation, the $(\mathrm{SEP})^2$ can be considered as a variance and, in a first approximation, can be analyzed as such. The Fisher-Snedecor test enables one to determine whether an SEP is significantly better than another SEP. If $(\mathrm{SEP})_0^2$ is the smallest $(\mathrm{SEP})^2$, every SEP such as:

$$F = \frac{(\mathrm{SEP})^2}{(\mathrm{SEP})_0^2} < F_c, \tag{6}$$

where F_c is the critical value provided by the Fisher-Snedecor tables for the number of degrees of freedom of the SEP. If $F < F_c$ (SEP) is not statistically significantly different (% of risk) from the SEP_0. F_c depends on this percentage of risk, generally set to 10%.[50]

RESULTS AND DISCUSSION

The functional properties of cassava starch films determined in this work in various thicknesses and starch concentration are presented in Table 1. The puncture force increased linearly ($R^2 = 0.97$), from 1.59 to 22.05 N, with the increasing of the film thickness, from 0.017 to 0.156 mm. These results are in agreement with those observed by Cuq[51] and Sobral,[39] who

Table 1. Reference values for the functional properties of cassava starch films

Sample	Thickness (mm)	Puncture force (N)	Puncture deformation (%)	WVP (g./hsmPa) 10^{-10}	Color difference	Opacity (%)
120	0.017	1.59	0.55	0.26	2.40	1.77
130	**0.022**	**2.83**	**0.56**	**0.38**	**2.37**	**1.89**
140	0.028	3.85	0.55	0.49	2.29	2.17
150	0.033	4.39	0.53	0.	2.43	2.44
160	0.039	5.31	0.64	0.71	2.79	1.89
170	0.044	6.34	0.62	0.66	2.72	2.60
220	0.028	3.35	0.56	0.36	2.09	2.07
230	0.038	5.07	0.58	0.	2.15	2.90
240	**0.049**	**6.83**	**0.64**	**0.81**	**2.20**	**3.00**
250	0.060	8.86	0.56	0.75	2.44	3.27
260	0.071	10.68	0.63	0.86	2.63	3.76
270	0.082	11.05	0.62	0.99	2.79	3.44
320	0.038	5.85	0.64	0.51	3.05	1.11
330	0.054	8.91	0.68	1.01	3.38	1.36
340	0.071	10.95	0.67	1.28	3.44	1.33
350	**0.087**	**14.27**	**0.74**	**1.06**	**3.78**	**1.39**
360	0.103	16.88	0.71	1.54	3.59	2.23
370	0.119	20.76	0.78	1.32	4.00	2.30
420	0.049	8.28	0.61	0.64	3.14	1.49
430	0.070	11.66	0.65	1.26	3.40	1.76
440	0.091	16.15	0.82	1.51	3.67	1.46
450	0.113	16.13	0.70	1.26	3.88	1.81
460	**0.134**	**20.19**	**0.88**	**1.32**	**4.29**	**2.06**
470	0.156	22.05	0.97	1.36	4.98	2.74

The samples noted in bold character were chosen for the prediction set.

worked with films of myofibrillar protein from the Atlantic sardine, gelatins and myofibrillar proteins from Nile Tilapia, respectively, using comparable thickness and identical puncture tests. Also, puncture deformation tended to increase linearly ($R^2 = 0.64$) with increasing of the film thickness differently to that observed by Cuq[49] and Sobral,[39] where puncture deformation remained practically constant, with an important dispersion of data.

The water vapor permeability (WVP) of starch cassava films also increased linearly ($R^2 = 0.75$) with the thickness from $0.26 \cdot 10^{-10}$ to $1.36 \cdot 10^{-10}$ g/m.sPa. Despite difficulty in explaining these results, this behavior was similar to that observed by Sobral[39] and McHugh.[52] On another side, the color difference ($R^2 = 0.81$) and opacity of films increased linearly with the increasing of film thickness, but the film opacity behaves in function of

starch concentration in FS: this effect was more important in the films with 1% and 2% ($R^2 = 0.83$) starch than in the films of 3% and 4% ($R^2 = 0.76$). Sobral[39] used the same techniques to measures these properties and observed that color difference increased with thickness but that opacity remained practically constant. More discussions about thickness influence on functional properties of cassava starch–based films are described in previous work.[18] On the other hand we can see in Table 1 that starch concentration is a very important factor. As a matter of fact, we can see important variations in the properties when the thickness is constant and for various concentrations.

Data Acquisition

The FTIR spectra of cassava starch and of its film in the region 1800–700 cm^{-1} are presented in Fig. 1. These spectra are similar to those observed in the work of Vandeerstraeten[53] and Demiate[33] that analyzed unmodified and chemically modified cassava starch. In general, both spectra seem to be similar, as cassava starch does not need plasticizer or other chemical agent to form film. But, in terms of band shape and intensity, some few differences may be observed in both spectra between 1100 and 900 cm^{-1} and around 1450 cm^{-1} (Fig. 1), typical of starch changing from semicrystalline to amorphous state.[54]

Around 1000 cm^{-1}, three separated bands can be seen in the spectrum of cassava starch: shape changes at 1042 cm^{-1} and 1015 cm^{-1}, and a peak at

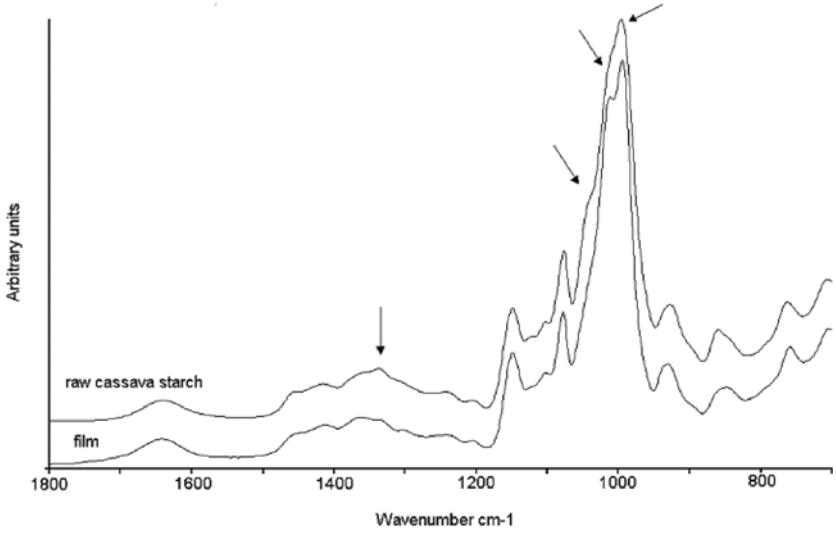

Figure 1. Examples of infrared spectra of cassava starch in powder and cassava starch film in the [1800–700] cm^{-1} spectral region.

996 cm^{-1}. These bands are sensitive to crystallinity, and the band at 1015 cm^{-1} was probably due to COH solvatation (Table 2). On the other hand, in the spectrum of cassava starch film, the band at 1042 cm^{-1} becomes less visible, and the position of the bands at 1015 cm^{-1} and 996 cm^{-1} shifted slightly to 1012 cm^{-1} and 994 cm^{-1}, respectively, and the band at 1012 cm^{-1} increased in intensity forming another peak. The band at 1015 cm^{-1} in starch spectrum is characteristic of amorphous material and is well visible in the spectrum of pregelatinized potato starch obtained by van Soest.[52] Thus, the change that occurred around 1000 cm^{-1} indicates that the starch film presents an amorphous structure.

According to Goodfellow,[28] in FTIR analysis of polysaccharides, the region of 1300–900 cm^{-1} is the domain more sensitive to molecular conformation. So, the observed change in bands between 1400 and 1300 cm^{-1} is probably not caused by differences in structure changes but to molecular

Table 2. Vibrational wavenumbers and assignments of infrared spectra of raw cassava starch and cassava starch films[26]

Wavenumber (cm^{-1})		
Raw starch	Starch film	Assignments
1642	1644	Water band
1455	1455	CH_2 bending in plane
1415	1412	
—	1362	
1337	1337	COH bending
—	1302	CH bending
1244	1242	CH_2OH related modes;
1207	1206	COH deformation;
1149	1149	C–O–C antisymmetric bridge stretching;
1123	1123	C–O–C vibrations;
1103	1102	COH stretching, antisymmetric in plane ring stretching;
1077	1078	
1042 (sh)	1042 (sh)	
1015 (sh)	1012	COH solvated
996	994	
927	931	Ring modes
860	—	
—	848	C(1)-H(α) bending modes
763	759	CH_2 rocking
707	704	

Definitions: sh = shoulder.

changes like CH and COH bending (Table 2) probably without implication on structure conformations.

Principal Component Analysis

In ATR spectra, the penetration depth of infrared light in the sample was about 0.2λ. In these conditions, we do not obtain any information about film thickness on the spectra. So we could study the functional properties of the starch film, using FTIR spectroscopy even if these properties are directly correlated with the film thickness. Principal component analysis was made in the fingerprint region, that is, in the band 1300–800 cm^{-1} of infrared spectra,[51] and used as a classification method in order to group samples with similar characteristics. The principal component of the data set explains 99% of the data matrix variance after extraction of three components. The further components contributed with less than 1% of the residual variance. It has been considered that components extracted after the third one model the non-significant variations as noise. Although the second principal component explained 7% of the total variance between the samples, this variance shows no important sample separation.

The scattergram of cassava starch films in the two directions PC1 and PC3 (Fig. 2) showed a separation into three groups, which can be correlated with the starch concentration in the filmogenic solution: zone 1, 1%; zone 2, 2%; and zone 3, 3% and 4%; the sample 470 appeared as outlier according with

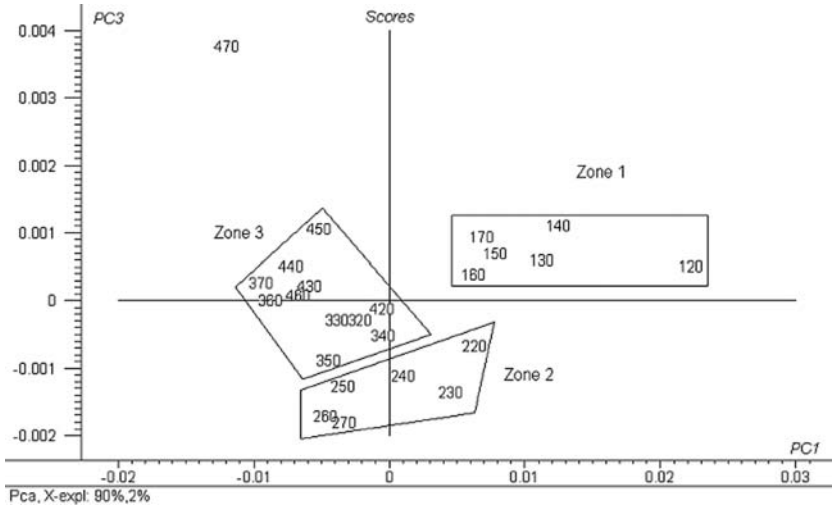

Figure 2. Distribution of samples in the space of the first and third principal component.

some of its properties as opacity. In each zone, the spectrum are projected as a function of the filmogenic solutions casted on the Plexiglas plate, which is correlated with the mechanical properties of films (puncture force or puncture deformation) (Table 1). These results demonstrate that there is enough information in the spectra, showing the relationship between the functional properties and structure of starch films. The infrared spectra may be used as an indicator of the functional properties of the films.

Prediction of Functional Properties

In order to find a relationship between the structure and the properties of polymer, we built a calibration between the IR spectra and each functional property (mechanical, optical, and barrier) using the PLS procedure. If the functional properties are related to structural changes in cassava starch films, the infrared spectra must contain some information relative to these modifications. The samples marked with an asterisk in Table 1 were tested on the prediction step, and the others were used to build the calibration set. For the building of the calibration, we used a full cross-validation method.

The results obtained in calibration and in prediction of each functional property analyzed, as a function of the number of factors included in the model, are given in Table 3. For each property, the Fisher-Snedecor test was used in order to know if there is any significant difference between the prediction results. The critical value F_c (3:3) given by the Fisher-Snedecor tables for 10% risk was 5.39. The comparison with the calculated F showed that the SEPs are statically equivalent for all properties. In such case, the factor number was chosen in function of the higher correlation coefficient. The examination of the relative error obtained in the prediction step showed that the functional properties could be modeled by the infrared spectra. The errors obtained were to be very important, but when these errors were related to the deviations on reference data (as seen above, 20% errors for the puncture force measurement) we can assume that the properties predicted with PLS modeling reproduced this deviation.

The regression vectors, which are conducive to better prediction results, present high contributions for the wavenumbers, highly correlated with the property of interest. The examination of these regression coefficients related to infrared spectra of films allows a better comprehension of the structure-properties relationship in the spectroscopic point of view.

The results of analyses of the puncture force and the puncture deformation presented regression coefficient very similar (Fig. 3a and 3b) with numerous contributions, and the higher ones are founded at 1240, 1012, and 994 cm^{-1} and close to the regression coefficient associated with the color determination (Fig. 3c). The regression coefficient obtained

Table 3. Optimization of the calibration model of the functional properties of cassava starch films. (SEC = standard error of calibration, SEP = Standard error of prediction, Cor = correlation coefficient)) The bold character indicates the final model used after the student test

	Puncture force (N)			Puncture deformation (%)			WVP $(g \cdot /s \cdot m \cdot Pa) \cdot 10^{-10}$		
Factor	SEC	SEP	Corr	SEC	SEP	Corr	SEC	SEP	Corr
1	2.884	3.490	0.929	0.071	0.085	0.906	**0.22**	**0.09**	**2.75**
2	2.313	2.956	0.970	0.049	0.086	0.920	0.20	0.12	2.67
3	**1.975**	**3.303**	**0.992**	**0.038**	**0.093**	**0.955**	0.19	0.14	2.71
4	1.398	3.172	0.972	0.035	0.098	0.881	0.15	0.15	2.55
5	1.245	3.030	0.980	0.033	0.093	0.946	0.14	0.12	2.76
6	0.884	2.733	0.983	0.274	0.100	0.835	0.11	0.23	2.52
7	0.729	2.737	0.966	0.022	0.090	0.781	0.08	0.28	2.32
8				0.020	0.089	0.783	0.07	0.33	1.87
Error (%)		29.94			13.19			10.73	
For the factor number in bold		(3)			(3)			(1)	

	Color			Opacity (%)		
Factor	SEC	SEP	Corr	SEC	SEP	Corr
1	0.474	0.601	0.817	0.717	0.598	−0.039
2	0.297	0.430	0.985	**0.662**	**0.438**	**0.908**
3	0.227	0.532	0.988	0.617	0.558	0.499
4	**0.164**	**0.521**	**0.993**	0.474	0.419	0.851
5				0.377	0.717	−0.750
6				0.270	0.617	−0.118
7				0.219	0.579	0.115
8				0.169	0.535	0.482
Error		16.48			21.01	
For the factor number in bold		(4)			(2)	

The line in bold character correspond to the factor number chosen.

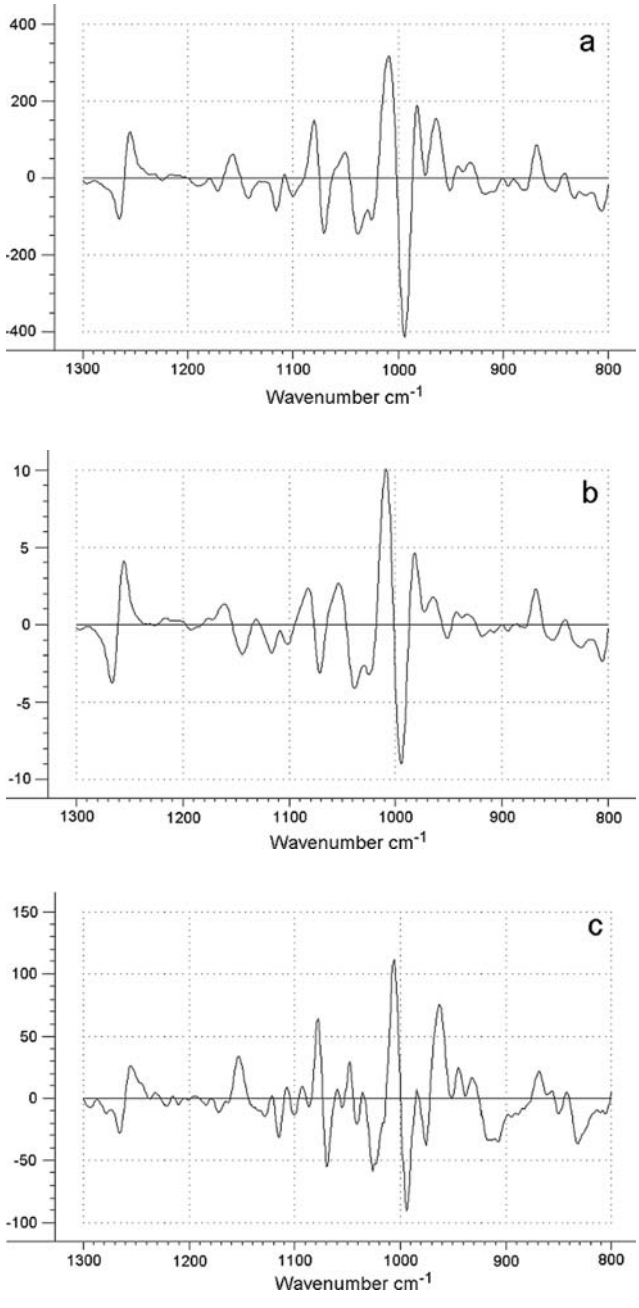

Figure 3. Regression coefficient of the functional properties of cassava starch films: puncture force (a), puncture deformation (b), color (c), opacity (d), water vapor permeability (e).

(*continued*)

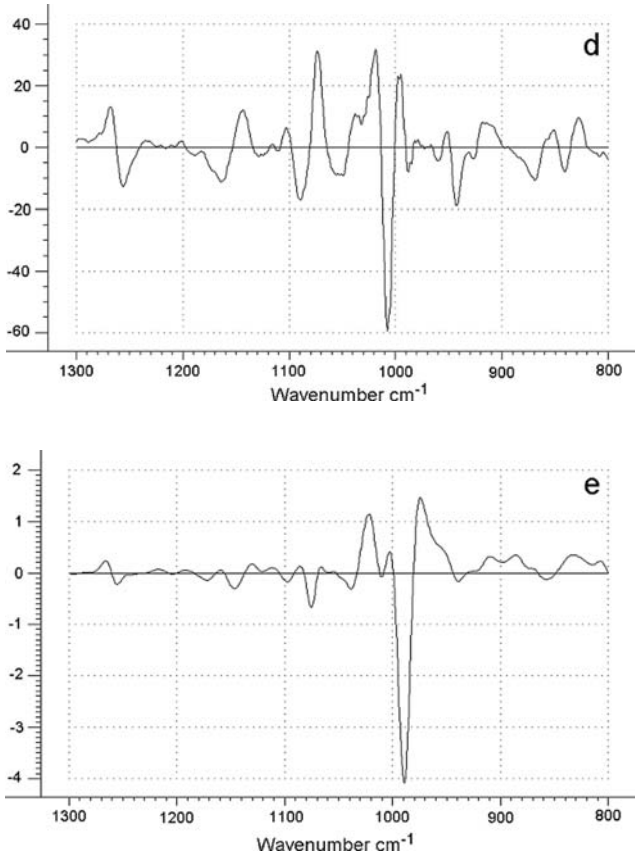

Figure 3. Continued.

for the determination of opacity (Fig. 3d) presents high contribution at 1240, 1070, 1049, 1012, 1008, 994, 940 cm^{-1}, and permeability (Fig. 3e) of film presents high contribution at 1070, 1020, 990, 970 cm^{-1}, respectively. All the properties of film seem to be correlated to the vibration bands at 994 and 1012 cm^{-1}. The opacity and the mechanical properties were related to the CH_2OH related modes at 1240 cm^{-1}, which could be attributed to the intermolecular cohesion. We could observe that the contribution of this band in all the regression coefficients present very high intensity compared to the one present in first-derived spectra of film (Fig. 4).

According to the assignment of the infrared spectra of starch film (Table 2), the band at 1012 cm^{-1} was attributed to COH solvated and that at 994 cm^{-1} was attributed to the intramolecular hydrogen bonding of the hydroxyl group on carbon 6 of the cyclic part of glucose, which is especially sensitive to the water content.[29]

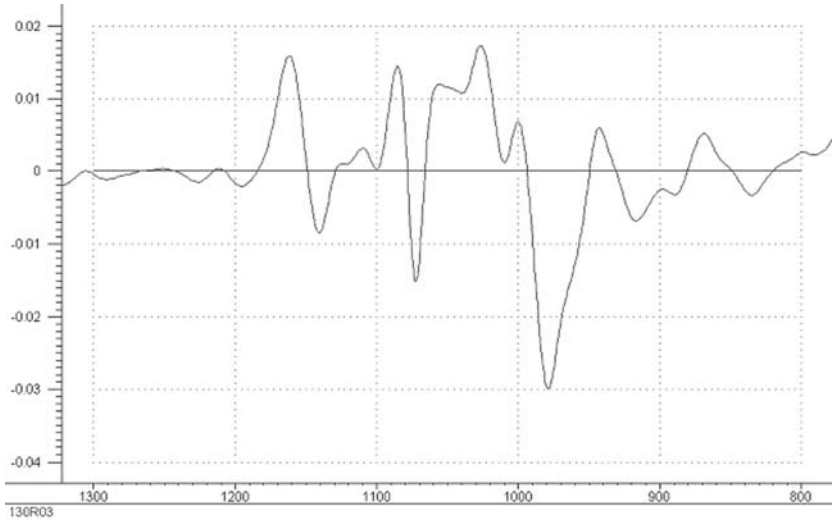

Figure 4. First derivative spectra of cassava starch film in the [1800–700] cm^{-1} spectral region.

CONCLUSIONS

The FTIR analysis of cassava starch and of its films shows few but important differences in both spectra. The spectrum of the native starch is characteristic of semicrystalline material, as expected. But, the spectrum of films is typical of amorphous starch, certainly due to thermal treatment of filmogenic solutions.

The PCA on FTIR–ATR spectra shows classification of the functional properties of cassava starch–based films in function of the concentration on starch in respective filmogenic solutions but does not distinguish the properties of films made with 3% and 4% of starch in FS.

The chemometric analysis shows that functional properties of cassava starch films are related to changes observed on the band around 1000 cm^{-1}, characteristics of changing systems from crystalline to amorphous state. In all cases, the intermolecular cohesion was important for the film properties according to the high contribution of the band at 1240 cm^{-1}.

ACKNOWLEDGMENTS

N.M.V, M.P.C., and P.J.A.S. would like to acknowledge CNRS, which allowed use of its laboratories (LASIR) for development of this research, and also FAPESP (Proc. 98/16179-8) for financial support. P.J.A.S. acknowledges CNPq (522953/95-6) for the research fellowship.

REFERENCES

1. Jokay, L.; Nelson, G. E.; Powell, E. L. Development of edible amylaceous coatings for foods. *Food Technol.* **1967**, *21* (8), 12–14.
2. García, M. A.; Martino, M. N.; Zaritzky, N. E. Plasticized starch-based coatings to improve strawberry (*Fragaria* x *Ananassa*) quality and stability. *J. Agri. Food Chem.* **1998**, *46* (9), 3758–3767.
3. Whistler, R. L.; Hilbert, G. E. Mechanical properties of films from amylose, amylopectin, and whole starch triacetates. *Indus. Eng. Chem.* **1944**, *36* (9), 796–798.
4. Wolff, I. A.; Davis, H. A.; Cluskey, J. E.; Gundrum, L. J.; Rist, C. E. Preparation of films from amylose. *Ind. Eng. Chem.* **1951**, *43* (4), 915–919.
5. Roth, W. B.; Mehltretter, C. L. Some properties of hydroxypropylates amylomaize starch films. *Food Technol.* **1967**, *21* (1), 72–74.
6. Ollett, A. L.; Parker, R.; Smith, A. C. Deformation and fracture behavior of wheat starch plasticized with glucose and water. *J. Mater. Sci.* **1991**, *26*, 1351–1356.
7. Nisperos-Carriedo, M. O. Edible coatings and films based on polysaccharides. In *Edible Coatings and Films to Improve Food Quality*; Krochta, J. M., Baldwin, E. A.; Technomic Publishing Company: Lancaster, 1994, pp. 305–335.
8. Lourdin, D.; Della Valle, G.; Colonna, P. Influence of amylose content on starch films and foams. *Carbohydr. Polym.* **1995**, *27* (4), 261–270.
9. Arvanitoyannis, I.; Nakayama, A.; Aiba, S. Edible films made from hydroxypropyl starch and gelatin and plasticized by polyols and water. *Carbohydr. Polym.* **1998**, *36*, 105–119.
10. Stading, M.; Rindlav-Westling, Å.; Gatenholm, P. Humidity-induced structural transitions in amylose and amylopectin films. *Carbohydr. Polym.* **2001**, *45*, 209–217.
11. Lazaridou, A.; Biliaderis, C. G. Thermophysical properties of chitosan, chitosan-starch and chitosan-pullulan films near the glass transition. *Carbohydr. Polym.* **2002**, *48*, 179–190.
12. Franco, C. M. L.; Daiuto, E. R.; Demiate, I. M.; Carvalho, L. J. C. B.; Leonel, M.; Cereda, M. P.; Vilpoux, O. F.; Sarmento, S. B. S. *Propriedades gerais do amido*; Fundação Cargill: Campinas, 2001; Vol. 1.
13. Vicentini, N. M.; Cereda, M. P. Uso de filmes de fécula de mandioca em pós-colheita de pepino (*Cucumis sativus* L.). *Brazilian J. Food Technol.* **1999**, *2* (1–2), 87–90.
14. Vicentini, N. M.; Castro, T. M. R.; Cereda, M. P. Influência de películas de fécula de mandioca na qualidade pós-colheita de frutos de pimentão (*Capsicum annuum* L.). *Ciência e Tecnologia de Alimentos* **1999**, *19* (1), 127–130.
15. Henrique, C. M.; Cereda, M. P. Utilização de biofilmes na conservação pós-colheita de morango (*Fragaria ananassa* Duch) cv. IAC Campinas. *Ciência e Tecnologia de Alimentos* **1999**, *19* (2), 231–233.
16. Chang, Y. P.; Cheah, P. B.; Seow, C. C. Plasticizing-antiplasticizing effects of water on physical properties of tapioca starch films in the glassy state. *J. Food Sci.* **2000**, *65* (3), 445–451.
17. Cereda, M. P.; Henrique, C. M.; Oliveira, M. A.; de, Ferraz, M. V.; Vicentini, N. M. Characterization of edible films of cassava starch by electron microscopy. *Brazilian J. Food Technol.* **2000**, *3*, 91–95.
18. Vicentini, N. M.; Sobral, P. J. A.; Cereda, M. P. *Plant Biopolymer Science: Food and Non-food Applications*; Renard, D., Della Valle, G., Popineau, Y., Eds.; Royal Society of Chemistry: Cambridge, 2002, pp. 291–300.

19. Wurzburg, O. B. *Modified Starches: Properties and Uses*; CRC Press Inc.: Boca Raton, 1986.
20. Gennadios, A.; Park, H. J.; Weller, C. L. Relative humidity and temperature effects on tensile strength of edible protein and cellulose ether films. *Trans. ASAE* **1993**, *36* (6), 1867–1872.
21. Bader, H. G.; Göritz, D. Investigations on high amylose corn starch films. Part 3: stress strain behaviour. *Starch/Stärke* **1994**, *46* (11), 435–439.
22. Lawton, J. W. Effect of starch type on the properties of starch containing films. *Carbohydr. Polym.* **1996**, *29*, 203–208.
23. Cuq, B.; Gontard, N.; Aymard, C.; Guilbert, S. Relative humidity and temperature effects on mechanical and water vapor barrier properties of myofibrillar protein-based films. *Polymer Gels Networks* **1997**, *5*, 1–15.
24. Rindlav-Westling, A.; Stading, M.; Hermansson, A. M.; Gatenholm, P. Structure, mechanical and barrier properties of amylose and amylopectin films. *Carbohydr. Polym.* **1998**, *36*, 217–224.
25. Anker, M.; Stading, M.; Hermansson, A. M. Relationship between the microstructure and the mechanical and barrier properties of whey protein films. *J. Agric. Food Chem.* **2000**, *48*, 3806–3816.
26. Galat, A. Study of the Raman and infrared absorption spectra of branched polysaccharides. *Acta Biochim. Polonica* **1980**, *27* (2), 135–142.
27. Wilson, R. H.; Goodfellow, B. J.; Belton, P. S.; Osborne, B. G.; Oliver, G.; Russell, P. L. Comparison of Fourier transform mid infrared spectroscopy and near infrared reflectance spectroscopy with differential scanning calorimetry for the study of the staling of bread. *Journal of the Science of Food and Agriculture* **1991**, *54*, 471–483.
28. Goodfellow, B. J.; Wilson, R. H. A Fourier transform IR study of the gelation of amylose and amylopectin. *Biopolymers* **1990**, *30*, 1183–1189.
29. van Soest, J. J. G.; de Wit, D.; Tournois, H.; Vliegenthart, J. F. G. Retrogradation of potato starch as studied by Fourier transform infrared spectroscopy. *Starch/Stärke* **1994**, *46* (12), 453–457.
30. Dolmatova, L.; Ruckebusch, C.; Dupuy, N.; Huvenne, J. P.; Legrand, P. Identification of modified starches using infrared spectroscopy and artificial neural network processing. *Appl. Spectrosc.* **1998**, *52* (3), 329–338.
31. Moya Moreno, M. C. M.; Mendoza Olivares, D.; Amezquita Lopez, F. J.; Gimeno Adelantado, J. V.; Bosh Reig, F. Determination of unsaturation grade and trans isomers generated during thermal oxidation of edible oils and fats by FTIR. *J. Mol. Structure* **1999**, *482–483*, 551–556.
32. Christy, A. A.; Egeberg, P. K.; Ostensen, E. T. Simultaneous quantitative determination of isolated trans fatty acids and conjugated linoleic acids in oils and fats by chemometric analysis of the infrared profiles. *Vib. Spectrosc.* **2003**, *32*, 37–48.
33. Demiate, I. M.; Dupuy, N.; Huvenne, J. P.; Cereda, M. P.; Wosiacki, G. Relationship between baking behavior of modified cassava starches and starch chemical structure determination by FTRI spectroscopy. *Carbohydr. Polym.* **2000**, *42*, 149–158.
34. Association of Official Analytical Chemists. Official Methods of Analysis of AOAC International (1995), 16th Ed.; AOAC International, Gaithersburg, MD.
35. Schoch, T. J.; Maywald, E. C. Preparation and properties of various vegetable starches. *Cereal Chem.* **1968**, *45* (6), 564–573.
36. Sobral, P. J. A.; Menegalli, F. C.; Hubinger, M. D.; Roques, M. A. Mechanical, water vapor barrier and thermal properties of gelatin based edible films. *Food Hydrocolloids* **2001**, *15*, 423–432.

37. Gontard, N.; Guilbert, S.; Cuq, J.-L. Water and glycerol as plasticizer affect mechanical and water vapor barrier properties of an edible wheat gluten film. *J. Food Sci.* **1993**, *58* (1), 206–211.
38. ASTM Standard. *Standard Test Methods for Water Vapor Transmission of Materials.* Annual book of ASTM standards. Designation E96-E80. Philadelphia: ASTM, 1989, pp. 730–739.
39. Hunterlab. *Universal Software Versions 3.2 and Above*. User's Manual. Manual Version 1.5; Hunter Associates Laboratory. Reston: Virginia, 1997.
40. Sobral, P. J. A. Propriedades funcionais de biofilmes de gelatina em função da espessura. *Ciência & Engenharia (Science & Engineering Journal)* **1999**, *8* (1), 60–67.
41. Sobral, P. J. A. Influência da espessura de biofilmes feitos à base de proteínas miofibrilares sobre suas propriedades funcionais. *Pesquisa Agropecuária Brasileira* **2000**, *32* (6), 1251–1259.
42. Martens, H.; Naes, T. *Multivariate Calibration*; Wiley: New York, 1989.
43. Dupuy, N.; Duponchel, L.; Amram, B.; Huvenne, J. P.; Legrand, P. Quantitative analysis of latex in paper coating by ATR-FTIR analysis. *Appl. Spectrosc.* **1994**, *8*, 333–347.
44. Millar, S.; Robert, P.; Devaux, M. F.; Guy, R. C. E.; Maris, P. Near-infrared spectroscopic measurements of structural changes in starch-containing extruded products. *Appl. Spectrosc.* **1996**, *50* (9), 1134–1139.
45. Martens, H. Factor analysis of chemical mixtures. *Anal. Chim. Acta* **1979**, *112*, 423–442.
46. Fuller, M. P.; Griffiths, P. R. Diffuse reflectance measurements by infrared Fourier transform spectrometry. *Anal. Chem.* **1978**, *50* (13), 1906–1910.
47. Haaland, D. M.; Thomas, E. V. Partial least-squares methods for spectral analysis. 1. Relation to other quantitative calibration methods and the extraction of qualitative information. *Anal. Chem.* **1988**, *60* (11), 1193–1202.
48. Liang, Y.-L.; Kvalheim, O. M. Robust methods for multivariate analysis - a tutorial review. *Chemometrics and Intelligent Laboratory Systems* **1996**, *32*, 1–10.
49. Savitzky, A.; Golay, M. J.E. Smoothing and differentiation of data by simplified least squares procedures. *Anal. Chem.* **1964**, *36*, 1627–1679.
50. Bauer, C.; Amram, B.; Agnely, M.; Charmot, D.; Sawatzki, J.; Dupuy, N.; Huvenne, J. P. On-line monitoring of a latex emulsion polymerization by fiber-optic FT-Raman spectroscopy. Part I: calibration. *Appl. Spectrosc.* **2000**, *54* (4), 528–535.
51. Cuq, B.; Gontard, N.; Cuq, J. L.; Guilbert, S. Functional properties of myofibrillar protein-based biopackaging as affected by film thickness. *J. Food Sci.* **1996**, *61* (3), 580–584.
52. McHugh, T. H.; Avena-Bustillos, R. J.; Krochta, J. M. Hydrophilic edible films: modified procedure for water vapor permeability and explanation of thickness effects. *J. Food Sci.* **1993**, *58* (4), 899–903.
53. Vandeerstraeten, F.; Wojciechowski, C.; Dupuy, N.; Huvenne, J. P. Reconnaissance de l'origine et des modifications d'amidons para traitement chimiométrique de données spectrales. *Analusis Magazine* **1998**, *26* (8), 57–62.
54. van Soest, J. J. G.; Tournois, H.; de Wit, D.; Vliegenthart, J. F. G. Short-range structure in (partially) crystalline potato starch determined with attenuated total reflectance Fourier transform IR spectroscopy. *Carbohy. Res.* **1995**, *279*, 201–214.